

Centralised distribution grid congestion management through EV charging control considering fairness and priority

Dreucci, Damiano; Yu, Yunhe; Chandra Mouli, Gautham Ram; Shekhar, Aditya; Bauer, Pavol

DOI

[10.1016/j.apenergy.2025.125417](https://doi.org/10.1016/j.apenergy.2025.125417)

Publication date

2025

Document Version

Final published version

Published in

Applied Energy

Citation (APA)

Dreucci, D., Yu, Y., Chandra Mouli, G. R., Shekhar, A., & Bauer, P. (2025). Centralised distribution grid congestion management through EV charging control considering fairness and priority. *Applied Energy*, 384, Article 125417. <https://doi.org/10.1016/j.apenergy.2025.125417>

Important note

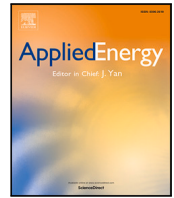
To cite this publication, please use the final published version (if applicable). Please check the document version above.

Copyright






Other than for strictly personal use, it is not permitted to download, forward or distribute the text or part of it, without the consent of the author(s) and/or copyright holder(s), unless the work is under an open content license such as Creative Commons.

Takedown policy

Please contact us and provide details if you believe this document breaches copyrights. We will remove access to the work immediately and investigate your claim.



Centralised distribution grid congestion management through EV charging control considering fairness and priority

Damiano Dreucci , Yunhe Yu , Gautham Ram Chandra Mouli *, Aditya Shekhar ,
Pavol Bauer 

Department of Electrical Sustainable Energy, Delft University of Technology, Mekelweg 4, Delft, 2628CD, The Netherlands

ARTICLE INFO

Keywords:

Congestion management
PTDF
Egalitarian
Fairness
Priority
Electric vehicle (EV)
Overload

ABSTRACT

To tackle the potential grid overloading issue induced by excessive Electric Vehicles (EV) charging demand, a Low Voltage (LV) grid congestion management algorithm with three centralised EV charging management schemes is proposed in this study. The developed algorithm integrates grid information and aims at tackling the foreseen congestion issues by operating on the EV charging processes. This is done through linear programming (LP) or iterative calculations. While the first charging scheme aims at managing the congestion by only affecting the elements with the greatest influence on the congestion, the other two aim at ensuring impartiality towards all users and the overall energy transfer to the EVs, respectively. The simulated results are compared in terms of performance criteria such as grid impact, user satisfaction and fulfilment of charging energy demand. Overall, this study shows that the first scheme brings the best results from a grid perspective. On the other hand, the last scheme leads to competitive results from a grid point of view and the best overall results from a user perspective.

1. Introduction

The global constant growth in the number of Electric Vehicles (EV) has led to the necessity of finding solutions to the technical issues that are expected to arise. One of these issues is the formation of overloads in the electrical grid due to the simultaneous charge of many EVs [1,2]. To study this phenomenon and to alleviate grid congestion problems, a centralised EV charging control algorithm is proposed in this study. Within this algorithm, one of three different Charging Management Schemes (CMS) can be integrated. These schemes define the logic for selecting charging stations where the charging power is adjusted and have been developed focusing on three different objectives. The first one aims at relieving the congestion by reducing the least total amount of power, the second one aims at distributing the power fairly among all charging stations, while the third option aims at optimising the success of the EV charging processes. These three CMSs are carried out via Linear Programming (LP) or iterative calculations. The algorithm is tested on two sub-urban Low Voltage (LV) distribution grid models with real grid data. In each grid, four different scenarios are simulated. In the first scenario, no CMS is applied. This is a reference case to assess the effects of uncontrolled EV charging. In the remaining scenarios, the algorithm is implemented by integrating one of the CMSs for each scenario. The results of these simulations are studied and compared in

terms of performance criteria, such as grid impact, user satisfaction and fulfilment of charging energy demand.

The methods to tackle grid congestion are generally categorised in literature into two major groups: Distribution Network Reconfiguration (DNR) [3,4] and Demand Response (DR) programs. Among DR, Direct Load Control (DLC) [5,6], economic mechanisms [7], or the combination of both [8] are commonly applied. The economic mechanism-based DR has a time scale from monthly, day-ahead to intra-day, while DLC aims at a very short term in the unit of minutes [9]. Moreover, DLC is more direct and accurate than the economic mechanism [10], making DLC a better candidate for the last-minute congestion management. To achieve the ideal congestion mitigation outcome, grid features often need to be incorporated in both the economic and the DLC approaches. For this reason, Distribution System Operators (DSO) usually play a key role in the process of grid congestion alleviation.

To avoid overburdening the aggregator's computational power, economic-based DR mechanisms increasingly incorporate new solutions. These solutions often integrate grid congestion information directly into the electricity market mechanism. Among these are Dynamic Tariff (DT), Dynamic Power Tariff (DPT) and Distribution Locational Marginal Price (DLMP). DLMP can be determined at each node by solving a DC optimal power flow (DCOPF) problem. This process often

* Corresponding author.

E-mail address: G.R.ChandraMouli@tudelft.nl (G.R. Chandra Mouli).

<https://doi.org/10.1016/j.apenergy.2025.125417>

Received 16 August 2024; Received in revised form 28 December 2024; Accepted 20 January 2025

Available online 10 February 2025

0306-2619/© 2025 The Authors. Published by Elsevier Ltd. This is an open access article under the CC BY license (<http://creativecommons.org/licenses/by/4.0/>).

employs the Power Transfer Distribution Factor (PTDF) concept to establish the relationship between node injection power and line power flow [11,12]. The DCOPF solution can also be used to calculate the DT. In [8] the DT is calculated by the DSO for market-based congestion management. Through DT the energy tariff is synchronised with the load demand magnitude. Finally, DPT is the power tariff with which the peak demand power of the customer is charged. In [7] DPT is used as a congestion signal and an OPF is executed at the DSO side to check the network limitations in which the PTDF is calculated. Nevertheless, the results obtained in [7,8,12,13] suggest that none of the congestion-adapted market methods solely can guarantee a stable congestion alleviation outcome. This is due to the stochasticity from the spot market price, the load demand and the behaviour of aggregators.

In order to efficiently access the local market or to calculate the congestion-coupled electricity tariff, the DSO needs to predict the spot market price as well as possess the whole knowledge of the load demand of the coming period [8,12,13]. On the other hand, for the transactive congestion mitigation algorithm, the more functionalities it incorporates (e.g., accounting for transformer overloading and voltage drop), the greater the number of iterations required for convergence. This will result in longer computational times to achieve price equilibrium [14]. To stabilise and improve the performance, the market mechanism method is usually combined with another market method [8], a grid reconfiguration [11,13] or another load response method to request extra flexibility through the DSO intervention [13,15]. However, cross-mechanism interactions, if not thoroughly examined in terms of financial charging schemes, grid flexibility assets, and weighing the temporal and locational factors of each mechanism, may pose risks to economic efficiency. They may also hinder the grid congestion alleviation. For instance, overlapping in grid congestion consideration across both mechanisms might lead to double charging or rewarding. Meanwhile, misalignment in temporal design could obstruct the effective simultaneous operation of both mechanisms. [16].

DLC methods could be a potential solution to the congestion issues. In [17] a decentralised Additive Increase and Multiplicative Decrease (AIMD) based EV charging method is proposed. In this the EV charging currents are controlled locally by referring to the local voltage fluctuations. The results showed that the AIMD-based method maintained the grid operation within the allowed constraints. A similar observation was made in [18], where the adaptive AIMD (A-AIMD) algorithm developed has excellent performance regarding transformer loading, charging fairness and user satisfaction. The centralised convex optimisation – whose objective is to maximise the EV charging power within the grid limits – outperforms the A-AIMD algorithm slightly. However, it is computationally heavy due to the grid power flow in its optimisation procedure. Therefore, a centralised grid congestion mitigation approach is more favourable regarding effectiveness and computational power saving. In this a central entity (e.g. DSO) oversees the grid operational condition and another entity like EV aggregator executes the DLC command. In the multi-objective congestion management algorithm developed in [19], the DSO is in charge of relieving any grid congestion through an interactive approach with the aggregators. During the interactive operation, the DSO uses PTDF to update the grid congestion level dependent Pareto weight, then the aggregator uses this weight to solve the multi-objective function. The PTDF can also be used as a very efficient way to identify the most congested branches, as well as to recognise through which buses the power injection has the highest impact on the congestion [20,21].

However, DLC could disturb the EV charging process substantially if grid congestion mitigation is the primary goal. Hence, EV user satisfaction is another key objective to consider while alleviating grid congestion through charging management. The expected EV connecting time and the requested departure State of Charge (SOC) are usually used to determine the charging urgency and hence the management of the charging processes [22,23]. How different priority criteria vary

the fairness in EV smart charging are extensively discussed in [24–26]. Paper [26] compares the power and time-coordinated charging methods in combination with three priority factors: SOC, slack time, and allotted time/energy. The results indicate that the combination of multiple priority criteria would achieve higher flexibility as well as fairness with different EV types. The fairness of EV smart charging is extended to the vehicle to grid (V2G) in research [24]. In this study, three EV management criteria are considered: the SOC level, the contribution to the V2G and the local load level. It is concluded that the contribution-based charging priority method can flatten the peak load while also shortening the EV charging time.

Following the above review and discussion, DLC appears to be a good candidate for accurate real-time grid congestion management, while PTDF is a great tool for identifying overloaded branches and their level of congestion. Rather than using PTDF to calculate the Available Transfer Capacity (ATC) or select suitable branches for DR, as most studies do, this paper uses PTDF differently. It leverages PTDF to determine how to adjust excessive EV charging demand to bring overloaded elements back to their normal operational range, while allowing for part of the load not to be met to ensure the grid is not congested. Besides, the above-reviewed EV-charging management research often concentrates on one main objective, which is to minimise EV user dissatisfaction or to improve the use of the grid. Conversely, this paper developed a PTDF-involved DLC congestion management algorithm combining with three EV CMSs focusing on efficacy, fairness and priority, respectively. Therefore, the main contributions of this paper can be summarised as follows:

- Developed a high-efficacy, centralised grid congestion recognition and mitigation algorithm with DLC mechanism involving PTDF. This algorithm allows to efficiently select the most appropriate EV charging processes to adjust, while also considering the degree to which they contribute to the congestion issues. The algorithm is combined with different EV Charging Management Schemes to demonstrate its efficacy. The proposed control method facilitates EV charging management but also allows for curtailment of EV load (if necessary) to ensure grid congestion is prevented.
- Three Charging Management Schemes have been developed, each with a distinct primary objective: congestion alleviation efficiency (aimed at reducing the least total amount of power), EV user fairness, and optimising the success of EV charging processes. Their performances have been compared, also in relation to an uncontrolled scenario where no congestion management scheme is included.
- Compared to earlier works, case studies were accomplished through grid simulation with two real grid models, as well as real measurement-based EV charging data. Simulation results were analysed from both DSO and user perspectives, including: branch overloading, voltage dip, EV charging demand satisfaction.
- The overcompensation phenomenon, which appears as an implication of the algorithm itself, is also extensively discussed.

The paper is organised as follows: methodology in Section 2; grid modelling and input data explanation, as well as scenario description are in Section 3; simulation results and analyses are presented in Section 4; while conclusion and recommendations are in Section 5.

2. Methodology

The proposed centralised algorithm shown in Fig. 1 adjusts the charging power at Electric Vehicle Supply Equipment (EVSE) to mitigate the grid congestion considering three possible schemes. These schemes are described in subsequent subsections: (i) PTDF-based Charging management Scheme (PCS) (ii) Egalitarian Charging management Scheme (ECS) (iii) Priority-based Charging management Scheme (PrCS). In the proposed algorithm architecture, the DSO detects whether grid congestions are bound to happen as a result of EV charging requests and

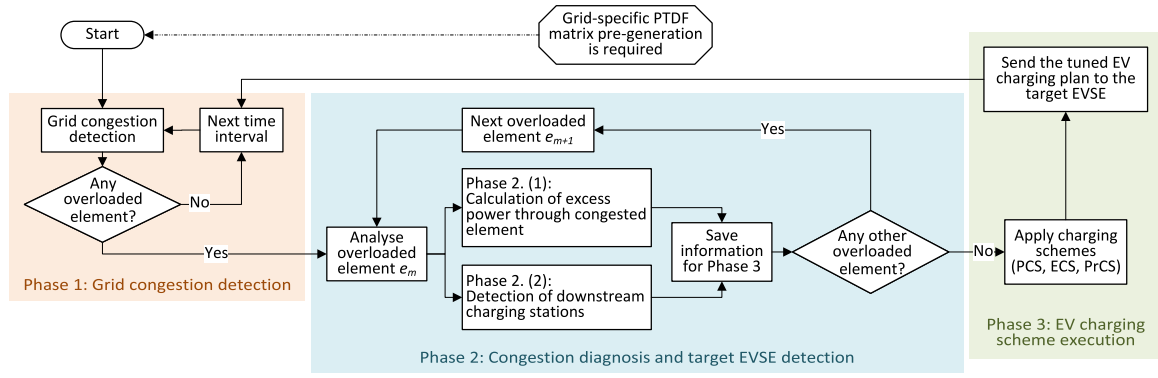


Fig. 1. Flowchart of the deployed algorithm.

sends the signal to the aggregators. This signal, in practice, represents a request for reduction or shift in charging power at specific points in time. This does not necessarily mean that EV charging processes are prematurely ended but are often only delayed within the EVs' parking duration. The aggregators and, in turn, the EV users would be compensated for their charging adjustments through agreements such as flexibility contracts.

The PTDF matrix is built by activating all EVSEs one at a time and registering the effects on all the other elements of the grid to indicate the variation in real power that occurs on all lines [27]. This is necessary to determine all EVSEs whose charging processes have an influence on the overloaded grid elements. It should be noted that only the nodes where an EVSE is connected have been included in the construction of the PTDF matrix. A fixed PTDF is considered consistent throughout the simulation, based on the assumption that the grid condition is stable and the node voltages can be maintained within expected boundaries [28]. Once the grid-specific PTDF matrix is built, the charging control algorithm is ready to be launched.

2.1. Phase 1: Grid congestion detection

The algorithm evaluates whether the current grid status, in conjunction with the EV charging requests, leads to congestion issues at a fixed time step in the scale of minutes. In a real operational environment, this could be done by checking the smart meter readings, communicating with the EV aggregators in combination with the background system simulation or distribution system estimation run by the DSO [29].

All the EVs' default charging requests at any given moment is set as uncontrolled, which is to charge at rated power, immediately after the EV is plugged in. In this study, congestion detection is realised through load flow analyses.

2.2. Phase 2: Congestion diagnosis and target EVSE detection

The main characteristics of the overloading issue are identified. These correspond to the problematic grid components such as the charging stations involved, along with their location and the magnitude of the issue. This phase consists of two main mechanisms that are discussed in the following subsections.

2.2.1. Calculation of excess power through congested elements

For M overloaded grid elements – $e_1, e_2, \dots, e_m, \dots, e_M$ – the excess power P_{em} of each overloaded element is estimated. The calculations shown here refer to the case of a congested line e_m , but the same logic applies in case the element is a transformer. The line loading percentage λ is given by (1).

$$\lambda = \frac{|I_{line}|}{I_r} \cdot 100 \quad (1)$$

where, I_{line} is the current registered at the line, while I_r is the rated current of the line. In case of a transformer, the same equation is

used at the low voltage and at the high voltage side, and the highest value is considered. The apparent phase power S_p – at any phase p – corresponding to the active (P_p) and reactive (Q_p) powers is given by (2).

$$S_p = \underline{U}_p \cdot \underline{I}_p^* = P_p + jQ_p \quad (2)$$

Where, the phase voltage U_p and the current I_p are written in terms of their complex representation in (3) and (4), respectively.

$$\underline{U}_p = U_{base}(u_{p,real} + ju_{p,imm}) \quad (3)$$

$$\underline{I}_p^* = I_{base}(i_{p,real} - ji_{p,imm}) = I_p(\cos\phi_i - jsin\phi_i) \quad (4)$$

Here U_{base} (in V) and I_{base} (in A) are the base voltage and current, respectively, while the term I_p (in A) refers to the magnitude of the current. The term ϕ_i refers to the current angle. The terms u_p and i_p are expressed in p.u.. Combining Eq. (3) and (4) with (2) and considering only the real part, P_p can be written as shown in (5).

$$P_p = U_{base}(u_{p,real}\cos\phi_i + u_{p,imm}\sin\phi_i)I_p = \bar{K}_{load}I_p \quad (5)$$

P_p can be rewritten in terms of λ in (6).

$$P_p = \frac{\lambda}{100}K_{load}I_r \quad (6)$$

For the maximum permitted power P'_p , the difference $\Delta P = P_p - P'_p$ should be reduced to resolve the overloading issue in phase p . Considering balanced operation, the three-phase excess power is calculated as $P_{em} = 3 \cdot \Delta P$ for each overloaded element e_m .

2.2.2. Detection of downstream charging stations

The second part of the process consists in collecting data regarding N EVSEs potentially available to have their charging power managed (labelled as $s_1, s_2, \dots, s_n, \dots, s_N$) and their influence on the congested elements of the network. This influence is described by matrix $\tilde{A}_{M,N}$ of size $M \times N$. The indices $a_{m,n}$ of matrix $\tilde{A}_{M,N}$ are directly derived from the PTDF matrix, and they indicate the percentage of power asked by charger s_n that flows through element e_m . The index $a_{m,n}$ in the matrix $\tilde{A}_{M,N}$ corresponds to the absolute value of the element at the intersection between charger s_n and the element e_m in the PTDF matrix. This case applies only if all the following conditions apply.

1. The flow of power caused by the EV is in the same power direction as the overloads.
2. Charging processes with an impact greater than a threshold of 5% on the congested element will be requested to have their charging power adjusted. Further details regarding the threshold selection and the influence of this number are provided in Section 4.4.
3. There is an EV connected currently asking for power at charging station s_n .

If any of the three options do not apply, the index $a_{m,n}$ will be set to zero.

2.3. Phase 3: EV charging scheme execution

The EV charging management scheme is activated, and from an uncontrolled charging start point, it determines which charging process to adjust at which EVSE to relieve the overloaded elements. Only one out of the three CMSs (PCS, ECS, PrCS) is used in this phase. It is important to note that this study does not account for variations in charging efficiency that may arise when the charging process deviates from the rated power.

2.3.1. PTFD-based charging management scheme (PCS)

The PCS optimally distributes the power to be reduced from relevant charging processes considering a grid point of view only. In fact, the only parameter included in the analysis to discern among the charging points is their influence on the overloaded elements. This information is contained in matrix $\tilde{A}_{M,N}$. Therefore, this scheme aims at reducing the minimum total amount of power possible, by operating on the chargers that contribute the most to the overload. This is made by means of a LP algorithm with an objective to maximise the power provided to the charging stations, as in Eq. (7).

$$\text{maximise } \sum_{n=0}^N P_{s_n}^{\text{new}} \quad (7)$$

The variables of the optimisation analysis are $P_{s_1}^{\text{new}}, P_{s_2}^{\text{new}}, \dots, P_{s_N}^{\text{new}}$, that are the charging power at EVSEs s_1, s_2, \dots, s_N , respectively, after the optimisation algorithm is applied. For these variables the following conditions apply:

$$P_{s_1}^{\text{new}}, P_{s_2}^{\text{new}}, \dots, P_{s_N}^{\text{new}} \geq 0 \quad (8)$$

$$P_{s_n}^{\text{new}} \leq P_{s_n}^{\text{ori}} \quad (9)$$

Where $P_{s_n}^{\text{ori}}$ represents the original power request at EVSE s_n before the charging scheme is executed.

The constraints are built so that all congestion issues are solved once the optimisation analysis is carried out. These constraints can be expressed in matrix notation as in Eq. (10). In this, the vector \bar{p}_s (11) contains the difference – at all EVSEs – between the original charging value and the new value after the optimisation (i.e. the optimisation variables). This is in practice the power to be reduced at each EV. On the other side of the inequality, \bar{p}_e (11) is a vector indicating the power that has to be reduced from the total power flowing through each congested element.

$$\tilde{A}_{M,N} \cdot \bar{p}_s \geq \bar{p}_e \quad (10)$$

where

$$\bar{p}_s = \begin{Bmatrix} P_{s_1}^{\text{ori}} - P_{s_1}^{\text{new}} \\ P_{s_2}^{\text{ori}} - P_{s_2}^{\text{new}} \\ \vdots \\ P_{s_N}^{\text{ori}} - P_{s_N}^{\text{new}} \end{Bmatrix} \quad \bar{p}_e = \begin{Bmatrix} P_{e_1} \\ P_{e_2} \\ \vdots \\ P_{e_M} \end{Bmatrix} \quad (11)$$

2.3.2. Egalitarian charging management scheme (ECS)

The ECS guarantees a fair absolute division of the burden among the chargers, disregarding any other aspect related with their influence on the congested elements or their need of power. The goal of the management scheme is to maximise the fairness of the reserve activation process, with a mechanism comparable to the one illustrated in [30]. As proved in that study, this charging management scheme also maximises social welfare and the Nash product of all EV users utilities.

In this case, the only variable is indicated as x ($x \geq 0$) and it can be described as the maximum charging power allowed at all EVSEs involved in the optimisation process. The objective is to maximise the variable x . The constraints are the same indicated in (10), but the vector

\bar{p}_s of the variables is described in (12):

$$\bar{p}_s = \begin{Bmatrix} P_{s_0}^{\text{ori}} - \min\{P_{s_0}^{\text{ori}}, x\} \\ P_{s_1}^{\text{ori}} - \min\{P_{s_1}^{\text{ori}}, x\} \\ \vdots \\ P_{s_N}^{\text{ori}} - \min\{P_{s_N}^{\text{ori}}, x\} \end{Bmatrix} \quad (12)$$

It should be noted that this optimisation analysis could be executed multiple times during the same time-step. This is done in order to avoid unnecessary power adjustments. In fact, if at the first iteration all the variables $P_{s_n}^{\text{new}}$ were set to the value x , all the overloading problems would indeed be solved. However, more power could have been reduced at the EVSEs than what was strictly necessary to solve the congestion.

To better explain this, it is important to consider that each constraint of the optimisation analysis represents a problem registered in the grid, namely an overloaded element. However, these problems are strongly interconnected. The same EV charging process(es) could be the common cause of multiple overloaded elements. Therefore, once the cause of an overloaded element has been addressed (through the reduction of power at one or multiple charging processes), other overloading issues could have been solved without the need of additional charging power reduction.

In practice, this is done by means of the concept of *Slack value* σ [31,32]. This represents the difference between the right and the left side of an inequality constraint, when the variable assumes a determined value. In other words, it is the value that returns an equality when added to the inequality constraint.

Once the optimisation analysis is solved, the introduction of the *Slack value* σ allows to rewrite (10) in the form of an equality, as $\tilde{A}_{M,N} \cdot \bar{p}_s = \bar{p}_e + \bar{\sigma}_e$. In combination with (12), these equalities can be written as in (13). Each line of this set of equations is indicated as C_e .

$$\begin{aligned} a_{1,1} \cdot (P_{s_1}^{\text{ori}} - \min\{P_{s_1}^{\text{ori}}, x\}) + \dots \\ + a_{1,N} \cdot (P_{s_N}^{\text{ori}} - \min\{P_{s_N}^{\text{ori}}, x\}) = P_{e_1} + \sigma_{e_1} \\ a_{2,1} \cdot (P_{s_1}^{\text{ori}} - \min\{P_{s_1}^{\text{ori}}, x\}) + \dots \\ + a_{2,N} \cdot (P_{s_N}^{\text{ori}} - \min\{P_{s_N}^{\text{ori}}, x\}) = P_{e_2} + \sigma_{e_2} \\ \vdots \\ a_{M,1} \cdot (P_{s_1}^{\text{ori}} - \min\{P_{s_1}^{\text{ori}}, x\}) + \dots \\ + a_{M,N} \cdot (P_{s_N}^{\text{ori}} - \min\{P_{s_N}^{\text{ori}}, x\}) = P_{e_M} + \sigma_{e_M} \end{aligned} \quad (13)$$

At each iteration, after the optimisation analysis is solved, the binding constraint C_b is taken. The binding constraint is in practice the one with *Slack value* equal to zero. The charging power of all EVSEs contained in this constraint is set to $\min\{P_{s_n}^{\text{ori}}, x\}$. This means that the overloading associated with constraint C_b is solved. Afterwards, it is checked whether also the other overloads, namely the remaining constraints, are solved. If so, the algorithm stops. Otherwise, it proceeds with the next iteration, where the previously binding constraint C_b is not considered anymore. The Pseudocode of the ECS scheme is listed in Algo. 1.

2.3.3. Priority-based charging management scheme (PrCS)

One of the key points of this method is the definition of a priority parameter, so to translate the urgency of power request of a charging session into a number. This number can be compared with the ones of the other charging stations and, when necessary, charging power at EVSEs will be adjusted accordingly. In particular, a *priority factor* can be defined for the charging session of the currently connected EV at charger s_n as

$$f_n = \frac{\Delta t_{\text{min},n}}{\Delta t_n} \quad (14)$$

where Δt_n is calculated as the difference $T_{d,n} - t$, with t representing the time of calculation and $T_{d,n}$ the expected departure time of the

Algorithm 1 Egalitarian Charging management Scheme (ECS)

```

1: done = False
2: while not done:
3:   run optimisation and get x
4:   if all Slack values are different than zero:
5:     done = True
6:   else:
7:     get constraint  $C_b$  with Slack value equal to zero
8:     set power at all chargers  $s$  present in  $C_b$ 
       at  $\min\{P_{s_n}^{ori}, x\}$ 
9:     remove constraint  $C_b$ 
10:  if power is set at all chargers in all constraints
11:  done = True

```

vehicle connected. The term $\Delta t_{min,n}$ refers instead to the minimum time necessary to complete the charging process and it is calculated as

$$\Delta t_{min,n} = \frac{d_{ch,n}}{P_{r,n}} \quad (15)$$

Where $d_{ch,n}$ is the remaining charging energy asked by the vehicle and $P_{r,n}$ is the rated charging power of the EV.

Similarly to one parameter in the work of Kumar et al. [26], the priority of charging is translated into f_n by comparing the minimum time necessary to complete the charging process with the actual time available. However, differently from [26], in this study no distinction is introduced between equivalent and minimum number of time steps required, and only the minimum time required at rated charging power is used. This priority factor f_n gives an indication of how urgent is the need of power at the studied element: the closer it gets to 1, the more urgent it needs power to charge its EV. In case $f_n > 1$, it will not be possible anymore to fully accomplish the original user charging demand. This parameter is used to decide which EVSE should be managed first to have their power reduced, in order to cause the least dissatisfaction possible. To do so, the EVSEs with a low f_n should have their charging power reduced first and the ones with a f_n close to 1 should not be reduced at all.

f_{dict} is defined as the dictionary that associates all EVs involved in the charging management process with their priority factors organised in increasing order. This can be obtained once all the output data from Phase 2 is collected. The description of this scheme can be found in [Algo. 2](#).

Algorithm 2 Priority-based Charging management (PrCS)

```

1: overloads = list of all overloaded elements
2: for  $s_n$  in  $f_{dict}$ :
3:   sub_overloads = sub-list of elements from
       overloads where corresponding value of  $s_n$ 
       in PTDF matrix is > 5%
4:   if sub_overloads not empty:
5:      $P_{s_n}^{new} = 0$ 
6:     create empty dictionary  $SOL_{dict}$ 
7:     for elem in sub_overloads:
8:        $SOL_{dict}[elem] = \text{True}$  if elem not
       overloaded anymore, checked via
       Eq. in (10)
9:   if all elem in  $SOL_{dict}$  are True:
10:    maximise  $P_{s_n}^{new}$  such that all elem
       in  $SOL_{dict}$  are still True
11:   for elem in sub_overloads:
12:     if  $SOL_{dict}[elem] = \text{True}$ :
13:       remove elem from overloads
14:   if overloads empty:
15:     break

```

3. Modelling of elements and scenarios**3.1. Grid features**

The congestion management algorithm has been coded in Python and tested via simulations on PowerFactory. The simulations have been run on two different LV grids. These are real Dutch sub-urban distribution grids provided by the DSO Enexis. Their main characteristics can be found in [Table 1](#).

All charging stations and regular loads included in the models are linked to nodes with a 3-phase connection. This simplification has been introduced in the model to increase the convergence ratio of the simulations, which otherwise resulted too complex to reach convergence at many time-steps. This assumption is in line with the intention of the authors not to include phase unbalance issues in the study, being it a distinct and extensive topic.

3.2. PV and load profiles

The baseload profile used for this study has been modelled on the base of the load characteristics included in the grid models, in combination with the Dutch normalised profiles [33]. These normalised profiles cover various connection types in different scales including household, business, agriculture and industrial usages. The load type as well as their yearly energy demand are provided in the original grid models.

To model the PV profile a previous study has been used as a base [34]. For both sub-urban grids used in this study a 15% PV penetration has been implemented, with a peak rated power of 2.5 kW assumed for each installation [35,36].

3.3. EV data

The EV data concerns two main aspects in particular: the charging behaviour of the EV users and the composition of the EV fleet, i.e. the electric vehicle models currently in circulation. Such a list of the most common EV models currently in circulation has been implemented on the base of the Dutch market data [37].

The EV charging behaviour includes all the key habits that can be registered of a EV user, such as EV arrival and departure time, charging energy request, and the frequency of the charging processes. This data is derived from a previous study that analyses the data of a significant number of charging sessions [38,39]. Based on the study, EV charging profiles are identified as home, semi-public and public charging featured sessions. In the case of a sub-urban grid, the percentage of home profile types represents 50% of the total sessions. The remaining half is equally divided between public and semi-public profiles. This is further described in [1]. The EV charging stations are modelled in PowerFactory as LV loads with a three-phase AC connections and a maximum of 32 A per phase.

The EV penetration is defined for each grid as the percentage of electric vehicles with respect to the total amount of vehicles registered. Different EV penetrations can be simulated by increasing the amount of EV charging sessions and, in turn, increasing the number of charging stations.

The detailed description of the grid models, and how the simulation data were generated can be found in previous works [1,2].

3.4. Simulation setups and scenarios

The simulations have been run by means of load flow analyses executed on intervals of 10 min. For each load flow the diagram in [Fig. 1](#) applies and provides an overview of the algorithm logic, as explained more in details in Section 2.

All the simulations to test the different CMSs have been run on the previously described models. In particular, eight different scenarios

Table 1
Summary of grids' characteristics.

Grid	No. households	Energy demand [MWh/y]	PV installed [kWp]	Avg. line length [m]	Longest feeder length [m]	No. transformer
1	475	1394.1	180	7.3	566.0	1 × 400 kVA
2	266	800.8	100	8.1	546.6	1 × 400 kVA

Table 2
Simulation scenarios and main results.

	CMS	λ_{trf}^{max} [%]	λ_{ln}^{max} [%]	δ_{max} [%]	R_{chr} [%]	R_{fail} [%]	E_{fail}^{avg} [kWh]	r_{chr} [%]	NNP
Grid 1: 50% EV penetration									
1	OFF	146.03	160.42	/	100	0	0	0	1
2	PCS	99.99	99.99	13.79	92.27	10.97	10.68	69.58	0.9230
3	ECS	100.04	99.93	8.38	94.34	12.65	6.76	44.04	0.9449
4	PrCS	100.15	99.94	18.84	99.79	4.00	0.44	2.87	0.9986
Grid 2: 100% EV penetration									
5	OFF	118.08	102.06	/	100	0	0	0	1
6	PCS	99.99	99.88	1.77	99.86	0.34	6.19	40.06	0.9983
7	ECS	100.00	95.01	1.74	99.93	0.80	1.35	8.74	0.9993
8	PrCS	100.00	99.56	2.54	99.99	0.11	0.02	0.13	1.0000

have been simulated, as detailed in Table 2. All the scenarios simulate an entire week in Winter, as the PV generation is lower and the EV impact on the grid was expected to be more significant.

The percentages of EV penetrations simulated in the two grids have been selected with the objective to simulate a congested grid condition. To this end, Grid 1 presented more severe loading conditions. In fact, it has been sufficient to increase the EV percentage to 50% in order to observe overloading phenomena up to 160% in the uncontrolled charging scenarios. On the other hand, for Grid 2 it has been necessary to increase the EV penetration up to 100% in order to register significant activations of the charging schemes. In this case, though, the maximum loading percentages observed always stayed below 120%.

4. Simulations results

In this section the simulation results are presented and analysed from three points of view: the grid congestion mitigation, the user satisfaction and the overcompensation of grid overloading. The overview of the overall performance of the three methods are listed in Table 2.

4.1. Grid congestion mitigation

The improvements to the grid performance brought by the three CMSs can be observed forthrightly with two main parameters: the maximum transformer loading (λ_{trf}^{max}) and the maximum line loading (λ_{ln}^{max}). For each time step, the loading of all transformers and lines are determined using Eq. (1) and then (λ_{trf}^{max}), (λ_{ln}^{max}) represent the highest loading recorded across all transformers and all lines in the grid, respectively. The maximum of these values registered during the whole week of simulation are reported in Table 2 as λ_{trf}^{max} and λ_{ln}^{max} , respectively.

It can be seen from Table 2 that all three CMSs managed to keep the loading percentages of both transformer and lines within the desired value of 100%. The maximum positive deviation observed is of 0.15% in the fourth scenario.

An overview of the results can also be observed in Fig. 2, which reports the effects on the maximum loading percentages registered at lines and at the transformer in grid 1. In particular, Fig. 2.B highlights the presence of a ‘valley filling’ effect. In fact, the high loading values registered in Scenario 1 – with peaks higher than 150% – are spread throughout the whole evening in the other 3 scenarios. In these the loading percentages are constantly below 100%. This can be also observed in Fig. 4.A, where the daily peak of EV power – greater than 200 kW – is moved to a later moment in the night.

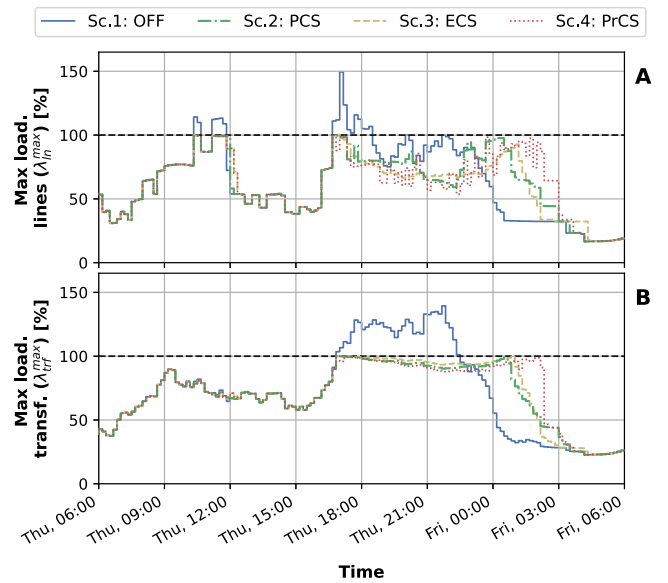


Fig. 2. Scenarios 1–4: comparison of max loading percentage at (A) lines and (B) transformer.

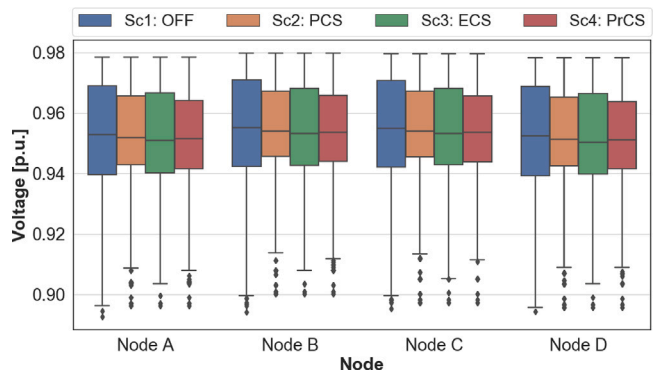


Fig. 3. Scenarios 1–4: comparison of voltage distribution at the three most distant nodes from the transformer, with a connection to: (A) home charging station, (B) public charging station, (C) semi-public charging station. Node (D) is the node with the lowest average voltage registered during the simulation of the uncontrolled scenario (Scenario 1).

The distribution of the node voltage of scenarios 1–4 are presented in the form of box plot in Fig. 3. In this graph four representative nodes are included.

From this graph it is possible to observe how the median value of the voltage decreases with the implementation of all CMSs. All three schemes kept the voltage less spread out, i.e. with lower inter-quartile ranges. In particular, the average value of this range for the four points considered is around 0.029 p.u. for the uncontrolled scenario, 0.026 p.u. for the ECS and around 0.022 p.u. for both PCS and PrCS. This can be explained as the integration of the algorithm of Fig. 1 – with any of the three CMSs – allows a better use of the available grid capacity. In contrast, in the uncontrolled scenarios, very low voltages are registered during peak hours – which lead to lower whiskers below 0.9 p.u. – while at all other moments very stable voltage conditions are present in the network. On the other hand, no significant effects are registered on the upper whiskers.

As expected, from a voltage point of view, the PCS is the solution that performed the best of all three charging management schemes. In fact, it led to the lowest inter-quartile range (together with PrCS). Besides, the PCS also resulted in the lowest drop in the median value, with respect to the uncontrolled scenario. The average drop in the median value registered at the four points considered is approximately 0.0011 p.u. for the PCS, against the drop of 0.0019 p.u. and 0.0014 p.u. for the ECS and the PrCS, respectively.

The scheme that registered the worst voltage results is the ECS. Next to registering the highest drop of the median value, it also shows the worst results in terms of lower whisker. The average lower whisker improvement – of all four points with respect to Scenario 1 – is 0.0072 p.u. for ECS, against 0.0135 p.u. for PCS and 0.0123 p.u. for PrCS.

4.2. User satisfaction

All three CMSs share the same fundamental mechanism, which is to reduce the excessive simultaneous charging request and delay the charging process as much as possible. By doing so the grid overloading is limited. However, the delayed charging process can also lead in some cases to a lower departure SOC for some EVs, with respect to the uncontrolled scenario. In fact, in the uncontrolled charging scenario the EVs get the maximum requested amount of energy technically obtainable during the parking time, disregarding all grid congestion issues that might occur.

One important aspect to consider is that whenever a charging process is adjusted to avoid grid congestion, the logic behind restricting one request instead of another will affect the satisfaction of EV owners. This section focuses on addressing the concept of fairness, using user satisfaction as a proxy quantitative parameter to fairness. It specifically examines one key question: to what extent has the charging of a limited number of EVs been restricted to ensure that all other requests are fulfilled? Or in other words, how evenly has the burden of resolving the congestion issue been distributed across the various charging stations?

In this study, the number of ‘failed charging process’ (J_{fail}) is defined as the absolute number of charging sessions performed by one of the three CMSs whose departure SOC is lower than the same session in the uncontrolled charging scenario. The charging energy received with uncontrolled charging strategy is considered as the ideal requested energy and is taken as a reference. In the following text, the term ‘requested energy’ is used.

The percentage of failed charging process (R_{fail}) is used to evaluate the user satisfaction and is reported for each scenario in Table 2. This percentage is calculated as the absolute number of failed charging process (J_{fail}) divided by the total number of EV charging processes simulated (J_{tot})

$$R_{\text{fail}} = \frac{J_{\text{fail}}}{J_{\text{tot}}} \quad (16)$$

Another criteria employed for user satisfaction assessment is the total delivered charging energy ratio R_{chr} . This is calculated as

$$R_{\text{chr}} = \frac{E_{\text{obt}}}{E_{\text{req}}} \quad (17)$$

where E_{req} refers to the sum of the requested energy of all EV charging processes simulated, while E_{obt} refers to the sum of the energy that was successfully provided during all charging processes. Therefore, it can be considered as a general indication of how the three CMSs performed in the simulated scenarios.

Looking at this last parameter from scenarios 2 to 4, the best results are obtained, in order, by: the PrCS (99.79%), the ECS (94.34%) and the PCS (92.27%). The same pattern is observed when considering scenarios 6 to 8, with percentages of total energy delivered of 99.99%, 99.93% and 99.86% for the PrCS, ECS and PCS, respectively.

However, looking into the details of what happens in the individual charging session, it is possible to make the following observations. The ECS case (scenarios 3 and 7) shows a higher total EV energy delivered (R_{chr}) than in the PCS case (scenarios 2 and 6). However, the former has a R_{fail} higher than the latter by 1.68% (comparing scenarios 2 and 3) and by 0.46% (comparing scenarios 6 and 7). In other words, the ECS has led to a higher percentage of failed charging processes with respect to the PCS.

This can be easily explained by looking at the last few columns of the table. The average failed energy of each scenario ($E_{\text{req}}^{\text{avg}}$) is calculated as

$$E_{\text{fail}}^{\text{avg}} = \frac{E_{\text{req}} - E_{\text{obt}}}{J_{\text{fail}}} \quad (18)$$

In the table it can be observed that the average failed energy is significantly higher in the PCS scenario with respect to the ECS (e.g. 10.68 kWh against 6.76 kWh for scenarios 2 and 3, respectively). The conclusion is that the ECS leads to a higher number of failed EV processes – which translates into a higher number of dissatisfied users – but with a lower dissatisfaction level for each user. This observation does not come unexpected, as the main purpose of the ECS is to distribute the burden of the charging power reduction as fairly as possible to the EVs. On the other hand, the PCS only looks at which charging stations allow to solve the overloading issue reducing the lowest amount of charging power possible. Therefore, the power adjustment burden is not shared fairly among charging stations and there is a higher chance that a smaller amount of EVs (with respect to the ECS) will see their charging process adjusted. The PrCS instead shows overall the best results, with a charging process failed percentage of 4.00% and an average failed energy of only 0.44 kWh for scenario 4. Similar observations can be made for scenarios 6 to 8.

The second to last column of Table 2 offers a clearer perspective on the average energy that has not been delivered during the failed charging processes (r_{chr}). This is calculated by dividing the average failed energy ($E_{\text{fail}}^{\text{avg}}$) of each scenario by the average requested energy of all charging processes that failed to be completed ($E_{\text{req, fail}}^{\text{avg}}$), as in

$$r_{\text{chr}} = \frac{E_{\text{fail}}^{\text{avg}}}{E_{\text{req, fail}}^{\text{avg}}} \quad (19)$$

The PCS scenarios show the most critical results, where this percentage reaches almost 70% in scenario 2 and slightly over 40% in scenario 6.

A final parameter to assess the fairness of the different CMSs is the Normalised Nashed Product (NNP) [30,40]. This parameter reflects the balance between competing interests and is independent of the scale of the individual utilities. This is used to assess the fairness of the energy distribution among all the EVs during the different charging processes, and is defined as

$$NNP = \sqrt{J_{\text{tot}} \prod_{j=1}^{J_{\text{tot}}} \frac{d_{\text{obt}, j}}{d_{\text{req}, j}}} \quad (20)$$

where $d_{req, j}$ represents the energy requested by the EV at each charging process j , while $d_{req, j}$ represents the total energy obtained by the EV before its departure. The value for each scenario is reported in Table 2. These findings align with the observations from previous parameters. From a user satisfaction standpoint, PrCS consistently delivers the best overall results. In terms of fairness, ECS does show improvements compared to PCS. However, its fairness performance remains inferior to that of PrCS. This leads to the conclusion that prioritising fairness in the short term (i.e., on a single time-step basis) does not result in the fairest distribution of energy over the long term.

4.3. Overcompensation of grid overloading

The main reason behind the outstanding performance of the PrCS is the fact that the charging stations with a more urgent need of energy are never requested to reduce their charging power if not strictly necessary. The urgency of the request is translated into a higher value of f_n , as in Eq. (14). On the other hand, the charging stations with lower f_n value are kept waiting so to give priority to the more urgent requests. Although following a different charging management scheme, also in the case of PCS and ECS some EVs are kept waiting or have their charging power adjusted when overload issues are registered.

A direct consequence of this approach is the formation of longer ‘waiting lines’, as it can be observed in Fig. 4.B. This can be observed through the average daily peak of waiting EVs, which is defined as the average of the daily maximum number of EVs simultaneously requesting charging power, calculated over the simulated week. The increase of this value with respect to Scenario 1 is 64.3%, 77.2% and 127.7% for Scenarios 2, 3 and 4, respectively. The same parameter increases for Scenarios 6, 7 and 8 – with respect to Scenario 5 – by 2.3%, 4.5% and 20.2%, respectively.

When considering the area below the curve of the number of active EVs, the increase of Scenarios 2, 3 and 4, with respect to Scenario 1 is 68.6%, 77.4% and 143.1%, respectively. A similar pattern, although less pronounced, is registered for Scenarios 6, 7 and 8, with respect to Scenario 5, with percentages of 1.7%, 1.9% and 7.5%, respectively.

The formation of these waiting lines can be viewed positively, as it helps maintain control over loading conditions by adjusting certain EV charging processes. On the other hand, this increase in the number of waiting EVs directly affects the performance of the CMSs. It can be observed in Fig. 2.B that the transformer loading value during peak hours of scenarios 2, 3 and 4 does not follow exactly the 100% line, but tends instead to create a valley shape. This is due to the fact that K_{load} (in Eq. (6)) is voltage dependent. The charging power to be reduced is calculated under voltage conditions that improve (increase) once the congestion issue in the network is actually solved. This improves in turn the loading condition of lines and transformer. This effect is more relevant when a significant amount of charging power is adjusted. This is visible in Table 2, where the value δ_{max} is reported in Eq. (21).

$$\delta_{max} = \max\{100 - \max\{\lambda_{trf}^{max}, \lambda_{ln}^{max}\}\}_{week} \quad (21)$$

This represents the maximum over-compensation phenomenon registered during the whole week of each simulation. Table 2 shows that the over-compensation phenomena in the simulations of Grid 2 is significantly lower than in Grid 1.

Similarly, in both grids there is a higher over-compensation presence in the scenarios where higher waiting lines form. The consequence is that, although all three strategies (PCS, ECS and PrCS) lead to the occurrence of overcompensation phenomena, this phenomenon is more present in the PrCS case. This means in practice that PCS and ECS allow to use the grid to a slightly fuller extent than PrCS (by following the 100% line more closely), although their overall performance appears to be lower than PrCS (as shown in Table 2).

The reduction of this overcompensation phenomenon by means of a correction factor resulted in inconsistent results depending on the

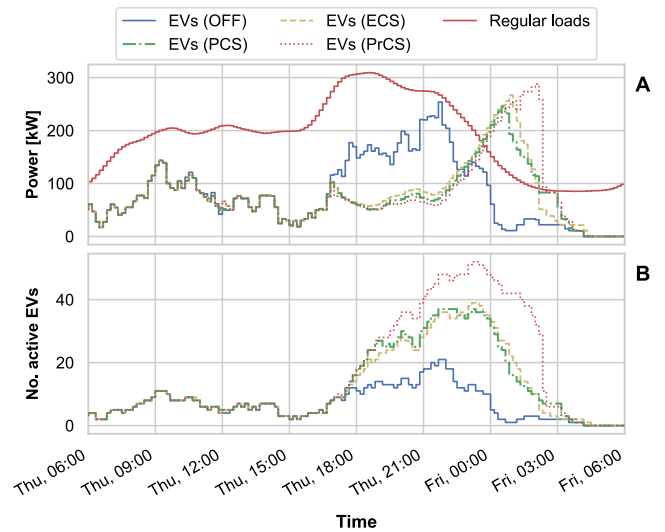


Fig. 4. Comparison of (A) registered EV power and (B) number of EVs requesting power to charge for scenarios 1–4.

magnitude and the exact location of the overloading issues. Therefore, no correction factor has been included in the algorithm. Another way to tackle the phenomenon is to integrate in the algorithm a correction mechanism that considers the effect on the voltage of the charging power adjustments. However, this is expected to add great complexity to the algorithm, which in turn, leads to a longer computational time.

4.4. Choice and effect of the threshold value for downstream charging stations

For this work, a threshold value of 5% was used for the detection of downstream charging stations. The decision of the threshold value should be regarded as a balance between a ‘regulatory’ choice and grid-specific considerations. For what concerns the regulatory aspect, the choice of a threshold value determines the contribution after which an EV is considered responsible to a congestion issue. On the basis of this, an EV will be taken into account when adjusting charging processes. For what concerns the grid specific considerations, the choice of a threshold value is severely dependent on the grid itself. Generally speaking, the values of the PTDF matrix tend to be more uniform and less extreme in a highly meshed grid as the power flows redistribute across multiple lines. Hence, a lower a threshold value can be selected for a highly meshed grid. The value of 5% was found to be a good balance between the regulatory choice (after which an EV is considered responsible for a congestion situation) and the grid-specific situation (a value that fits with the topology of both grids studied).

Regarding the sensitivity of the threshold value:

- In the case of PCS, no significant change in the results is observable at the change of the threshold value. This is because the algorithm selects only the chargers with the greatest influence on the congested elements (i.e. with the highest PTDF values associated).
- In the case of ECS and PrCS, the higher the threshold value, the closer the performance of the algorithms to the PCS. Setting a higher threshold value forces the algorithm to operate only on the charging processes with the greatest influence on the congestion issues (which is the main objective of PCS).
- In the case of ECS and PrCS, lowering the threshold distributes the ‘burden’ more equally to solve the congestion issue among more EVs (even to those with very little influence on it). This makes the congestion management less efficient (as more total power needs

to be curtailed to solve the same congestion issue). However, the user satisfaction is more equally distributed as well.

5. Conclusion and recommendations

Correctly managing the EV charging processes can be a key element to prevent the occurrence of congestion issues in the grid, while still delivering the required energy to the vehicles. In this study, a PTDF-based congestion mitigation algorithm has been developed to maintain the loading conditions of a congested grid within the desired limits. This was used in combination with three charging management schemes, which have all been tested and compared. The activation of all three schemes was successful to solve overloading conditions at both the transformer and the lines, with a negligible error. Their integration also led to a better use of the available grid capacity, which affected, in turn, the voltage distribution in the network. However, the different objectives of the three management schemes resulted in different outcomes for what concerns the user satisfaction. When comparing the ECS with the PCS, the conclusion is that the former leads to higher number of dissatisfied users with respect to the latter, but with a lower dissatisfaction level for each user. This is in line with the objective of the ECS algorithm to maximise fairness. On the other hand, the PCS is the scheme that resulted in the highest average charging energy that was failed to be delivered, both in absolute and relative terms. Overall, the PrCS is the scheme that performed the best, with the lowest percentages of failed charging processes and the greatest total delivered charging energy ratio. From a fairness perspective, this leads to the conclusion that PrCS also delivered the fairest distribution of energy over the long term.

Finally, it was observed a significant growth in the volume of the EV ‘waiting lines’ with respect to the uncontrolled scenarios. This increase was comparable for the PCS and ECS cases, while it was significantly higher for the PrCS. The direct consequence of the longer waiting lines is an increase in the overcompensation phenomena. Although this aspect did not impede to reach the main objective of the algorithm – i.e. to keep the loading percentages within the allowed limit – their presence suggests that the available grid capacity has not been exploited to the fullest. The reduction of this phenomenon will be the starting base for the future work.

Another point of interest concerns the threshold value used to determine which charging stations are considered during the congestion management process. In this study, a value of 5% was used. This is regarded as a good balance between the ‘regulatory’ choice, to select which EVs are considered responsible for a congestion issue, and the conditions of the specific grids selected in this study. In future studies it would be interesting to run a sensitivity analysis to find the optimal value and see how this varies by comparing different highly meshed grids. Furthermore, this algorithm evaluates the charging requests of the EVs at each time-step. In future work, a different mechanism could be implemented where EVs follow the assigned optimal charging profile until a new command is sent to further save computational power. This new signal could be sent when there is a relevant system status change. Finally, this algorithm aims at preventing the occurrence of congestion issues before they happen, but the same schemes could also be applied as a remedial action to solve congestion issues that have already been registered in the grid. This aspect could also be evaluated in future work.

CRedit authorship contribution statement

Damiano Dreucci: Writing – original draft, Methodology, Formal analysis, Conceptualization. **Yunhe Yu:** Writing – original draft, Validation, Methodology. **Gautham Ram Chandra Mouli:** Writing – review & editing, Supervision, Project administration. **Aditya Shekhar:** Writing – review & editing, Validation. **Pavol Bauer:** Writing – review & editing, Supervision, Resources.

Declaration of competing interest

The authors declare the following financial interests/personal relationships which may be considered as potential competing interests: Yunhe Yu reports financial support was provided by ERA-NET Cofund Electric Mobility Europe (EMEurope). Yunhe Yu reports equipment, drugs, or supplies was provided by Dutch DSO Enexis. If there are other authors, they declare that they have no known competing financial interests or personal relationships that could have appeared to influence the work reported in this paper.

Data availability

The authors do not have permission to share data.

References

- [1] Yu Y, Shekhar A, Mouli GCR, Bauer P, Refa N, Bernards R. Impact of uncontrolled charging with mass deployment of electric vehicles on low voltage distribution networks. In: 2020 IEEE transportation electrification conference expo. ITEC, 2020, p. 766–72. <http://dx.doi.org/10.1109/ITEC48692.2020.9161574>.
- [2] Yu Y, Reihns D, Wagh S, Shekhar A, Stahleder D, Mouli GRC, et al. Data-driven study of low voltage distribution grid behaviour with increasing electric vehicle penetration. *IEEE Access* 2022;1–18. <http://dx.doi.org/10.1109/ACCESS.2021.3140162>.
- [3] Zhang X, Liu Y, Gao H, Wang L, Liu J. A bi-level corrective line switching model for urban power grid congestion mitigation. *IEEE Trans Power Syst* 2020;35(4):2959–70. <http://dx.doi.org/10.1109/TPWRS.2019.2959586>.
- [4] Bouhours AS, Christoforidis GC, Parissis C, Labridis DP. Reducing network congestion in distribution networks with high dg penetration via network reconfiguration. In: 11th international conference on the European energy market (EEM14). 2014, p. 1–5. <http://dx.doi.org/10.1109/EEM.2014.6861255>.
- [5] Shabshab SC, Lindahl PA, Nowocin JK, Donnal J, Blum D, Norford L, et al. Demand smoothing in military microgrids through coordinated direct load control. *IEEE Trans Smart Grid* 2020;11(3):1917–27. <http://dx.doi.org/10.1109/TSG.2019.2945278>.
- [6] Zhang L, Tang Y, Zhou T, Tang C, Liang H, Zhang J. Research on flexible smart home appliance load participating in demand side response based on power direct control technology. *Energy Rep* 2022;8:424–34. <http://dx.doi.org/10.1016/j.egyr.2022.01.219>.
- [7] Huang S, Wu Q, Shahidehpour M, Liu Z. Dynamic power tariff for congestion management in distribution networks. *IEEE Trans Smart Grid* 2019;10(2):2148–57. <http://dx.doi.org/10.1109/TSG.2018.2790638>.
- [8] Fotouhi Ghazvini MA, Lipari G, Pau M, Ponci F, Monti A, Soares J, et al. Congestion management in active distribution networks through demand response implementation. *Sustain Energy, Grids Networks* 2019;17:100185. <http://dx.doi.org/10.1016/j.segan.2018.100185>.
- [9] Dranka GG, Ferreira P. Review and assessment of the different categories of demand response potentials. *Energy* 2019;179:280–94. <http://dx.doi.org/10.1016/j.energy.2019.05.009>.
- [10] Gong X, Castillo-Guerra E, Cardenas-Barrera JL, Cao B, Saleh SA, Chang L. Robust hierarchical control mechanism for aggregated thermostatically controlled loads. *IEEE Trans Smart Grid* 2021;12(1):453–67. <http://dx.doi.org/10.1109/TSG.2020.3009989>.
- [11] Zhao J, Wang Y, Song G, Li P, Wang C, Wu J. Congestion management method of low-voltage active distribution networks based on distribution locational marginal price. *IEEE Access* 2019;7:32240–55. <http://dx.doi.org/10.1109/ACCESS.2019.2903210>.
- [12] Liu Z, Wu Q, Oren SS, Huang S, Li R, Cheng L. Distribution locational marginal pricing for optimal electric vehicle charging through chance constrained mixed-integer programming. *IEEE Trans Smart Grid* 2018;9(2):644–54. <http://dx.doi.org/10.1109/TSG.2016.2559579>.
- [13] Shen F, Huang S, Wu Q, Repo S, Xu Y, Østergaard J. Comprehensive congestion management for distribution networks based on dynamic tariff, reconfiguration, and re-profiling product. *IEEE Trans Smart Grid* 2019;10(5):4795–805. <http://dx.doi.org/10.1109/TSG.2018.2868755>.
- [14] Hu J, Yang G, Bindner HW, Xue Y. Application of network-constrained transactive control to electric vehicle charging for secure grid operation. *IEEE Trans Sustain Energy* 2017;8(2):505–15. <http://dx.doi.org/10.1109/TSTE.2016.2608840>.
- [15] Asrari A, Ansari M, Khazaei J, Fajri P. A market framework for decentralized congestion management in smart distribution grids considering collaboration among electric vehicle aggregators. *IEEE Trans Smart Grid* 2020;11(2):1147–58. <http://dx.doi.org/10.1109/TSG.2019.2932695>.

- [16] Ormeño-Mejía E, Chaves-Ávila JP, Troncia M. Unlocking flexibility from third-party resources: Decoding the interaction between mechanisms for acquiring distribution system operator services. *Curr Sustainable/ Renew Energy Rep* 2024;11:45–67. <http://dx.doi.org/10.1007/s40518-024-00236-7>.
- [17] Ucer E, Kisacikoglu MC, Yuksel M. Decentralized additive increase and multiplicative decrease-based electric vehicle charging. *IEEE Syst J* 2021;15(3):4272–80. <http://dx.doi.org/10.1109/JSYST.2020.3013189>.
- [18] Zishan AA, Haji MM, Ardakanian O. Adaptive congestion control for electric vehicle charging in the smart grid. *IEEE Trans Smart Grid* 2021;12(3):2439–49. <http://dx.doi.org/10.1109/TSG.2021.3051032>.
- [19] Khan OGM, Youssef A, Salama M, El-Saadany E. Robust multi-objective congestion management in distribution network. *IEEE Trans Power Syst* 2022;1–11. <http://dx.doi.org/10.1109/TPWRS.2022.3200838>.
- [20] Dehnavi E, Afsharnia S, Akmal AAS, Moeini-Aghaie M. A novel congestion management method through power system partitioning. *Electr Power Syst Res* 2022;213:108672. <http://dx.doi.org/10.1016/j.epsr.2022.108672>.
- [21] Baczynska A, Niewiadomski W. Power flow tracing for active congestion management in modern power systems. *Energies* 2020;13(18). <http://dx.doi.org/10.3390/en13184860>.
- [22] Prakash K, Ali M, Siddique M, Karmaker A, Macana C, Dong D, et al. Bi-level planning and scheduling of electric vehicle charging stations for peak shaving and congestion management in low voltage distribution networks. *Comput Electr Eng* 2022;102:108235. <http://dx.doi.org/10.1016/j.compeleceng.2022.108235>.
- [23] Liu L, Zhou K. Electric vehicle charging scheduling considering urgent demand under different charging modes. *Energy* 2022;249:123714. <http://dx.doi.org/10.1016/j.energy.2022.123714>.
- [24] Xie S, Zhong W, Xie K, Yu R, Zhang Y. Fair energy scheduling for vehicle-to-grid networks using adaptive dynamic programming. *IEEE Trans Neural Networks Learn Syst* 2016;27(8):1697–707. <http://dx.doi.org/10.1109/TNNLS.2016.2526615>.
- [25] Zeballos M, Ferragut A, Paganini F. Proportional fairness for EV charging in overload. *IEEE Trans Smart Grid* 2019;10(6):6792–801. <http://dx.doi.org/10.1109/TSG.2019.2911231>.
- [26] Kumar KN, Sivaneasan B, So PL. Impact of priority criteria on electric vehicle charge scheduling. *IEEE Trans Transp Electrification* 2015;1(3):200–10.
- [27] Cheng X, Overbye T. PTDF-based power system equivalents. *IEEE Trans Power Syst* 2005;20(4):1868–76. <http://dx.doi.org/10.1109/TPWRS.2005.857013>.
- [28] Baldick R. Variation of distribution factors with loading. *IEEE Trans Power Syst* 2003;18(4):1316–23. <http://dx.doi.org/10.1109/TPWRS.2003.818723>.
- [29] Ahmad F, Rasool A, Ozsoy E, Sekar R, Sabanovic A, Elitaş M. Distribution system state estimation-a step towards smart grid. *Renew Sustain Energy Rev* 2018;81:2659–71. <http://dx.doi.org/10.1016/j.rser.2017.06.071>.
- [30] Hekkelman B, la Poutré H. Fairness in smart grid congestion management. In: 2019 IEEE PES innovative smart grid technologies europe (ISGT-europe). 2019, p. 1–5.
- [31] Boyd S, Vandenberghe L. *Convex optimization*. Cambridge University Press; 2004, p. 131, URL https://web.stanford.edu/~boyd/cvxbook/bv_cvxbook.pdf.
- [32] Matoušek J, Gärtner B. *Understanding and using linear programming*. vol. 1, Berlin: Springer; 2007, p. 42.
- [33] verbruiksprofielen-Profielen 2018. De Vereniging Nederlandse EnergieDataUitwisseling (NEDU); 2021, (Accessed 20 April 2021). URL <https://www.nedu.nl>.
- [34] Mouli GC, Bauer P, Zeman M. System design for a solar powered electric vehicle charging station for workplaces. *Appl Energy* 2016;168:434–43.
- [35] Zonnestroom; vermogen bedrijven en woningen, regio(indeling 2018),2012–2018. Centraal Bureau voor de Statistiek; 2021, (Accessed 20 April 2021). URL <https://opendata.cbs.nl>.
- [36] Factsheets Zon. Rijksdienst voor Ondernemend Nederland (RVO); 2021, (Accessed 20 April 2021). URL <https://www.rvo.nl>.
- [37] Statistics Electric Vehicles and Charging in The Netherlands up to and including November 2018. Rijksdienst voor Ondernemend Nederland (RVO); 2021, (Accessed 20 April 2021). URL <https://www.rvo.nl>.
- [38] Elaad open data platform, 2018. Elaad; 2021, (Accessed 11 May 2021).
- [39] Refa N, Nick H. Impact of smart charging on EVs charging behaviour assessed from real charging events. Lyon, France: 32th International Electric Vehicle Symposium; 2019.
- [40] Nash J. The bargaining problem. vol. 18, (2):Wiley Online Library; 1950, p. 155–62,